

Enigmatic Velocity Dispersions of Ultra-Diffuse Galaxies in Light of Modified Gravity Theories and Radial Acceleration Relation

Tousif Islam^{1,*}

¹ Center for Scientific Computation and Visualization Research (CSCVR),
University of Massachusetts (UMass) Dartmouth, Dartmouth, MA-02740, USA

Recent observations of anomalous line-of-sight velocity dispersions of two ultra-diffuse galaxies (UDGs) provide a stringent test for modified gravity theories. While NGC 1052-DF2 exhibits an extremely low dispersion value ($\sigma \sim 7.8_{-2.2}^{+5.6}$ km/s), the reported dispersion value for NGC 1052-DF44 is quite high ($\sigma \sim 41.0 \pm 8$ km/s). For DF2, the dynamical mass is almost equal to the luminous mass suggesting the galaxy have little to no ‘dark matter’ in Λ CDM whereas DF44 requires a dynamical mass-to-light ratio of ~ 30 making it to be almost entirely consists of dark matter. It has been claimed that both these galaxies, marking the extreme points in terms of the estimated dynamical mass-to-light ratio among known galaxies, would be difficult to explain in modified gravity scenarios. Extending the analysis presented in [1], we explore the dynamics of DF2 and DF44 within the context of three popular alternative theories of gravity [Modified Newtonian Dynamics (MOND), Weyl Conformal gravity and Modified gravity (MOG)] and examine their viability against the dispersion data of DF2 and DF44. We then demonstrate the possible diversities in the dispersion profiles of UDGs that modified gravity theories can accommodate. We further show that the galactic ‘Radial Acceleration Relation’ (RAR) is consistent with DF44 dispersion data but not with DF2.

I. INTRODUCTION

van Dokkum et al [2–4] have recently reported two ultra-diffuse galaxies (UDGs), NGC 1052-DF2 and NGC 1052-DF4, having extraordinarily low velocity dispersions of $\sigma \sim 7.8_{-2.2}^{+5.6}$ km/s. and $\sigma \sim 4.2_{-2.2}^{+4.4}$ km/s respectively. The inferred total dynamical mass of both the galaxies is $\sim 2.0 - 3.0 \times 10^8 M_\odot$ (where M_\odot is the solar mass) which is almost equal to the luminous mass of these galaxies [2–4]. The authors therefore suggested that these two galaxies are dominated by baryons and lack dark matter. They further claimed that the absence of dark matter (or, in other words, the low velocity dispersions) would be extremely difficult to explain in any modified theory of gravity which tries to explain the observed ‘mass discrepancies’ in galaxies and clusters through modification of the laws of gravity without invoking the existence of the apparent ‘dark matter’. The discovery of DF2 (and DF4) become extremely significant when they are compared with another UDG named NGC 1052-DF44 [5] whose morphology and mass contents are similar to DF2 (and DF4) but exhibits a relatively high velocity dispersions ($\sigma \sim 41.0 \pm 8$ km/s) indicating the galaxy to be dark matter dominated. Thus, these two UDGs represent the extreme ends of the relative baryon and dark matter contents in a particular galaxy. While, in Λ CDM (general relativity with dark matter and dark energy), these galaxies might be easier to account for, their formation channel remains poorly understood [6–9]. For modified gravity theories, it is not immediately clear whether they would be able to explain the anomalous velocity dispersions of both the galaxies. Thus these two galaxies provide an acid test for any modified gravity.

We also note that the dynamics of hundreds of galaxies are well known to follow a phenomenological relation called ‘Radial Acceleration Relation’ (RAR) [10] which is regarded to be an indication of the breakdown of the Newtonian gravity (and consequently of general relativity in its weak field limit) at the galactic scale. Given DF2 and DF44 have defied the current understanding of the galaxy rotation curves and the

standard stellar-to-halo-mass ratio [11], it is important to look into whether the dynamics of DF2 and DF44 are consistent with RAR.

In this paper, we therefore present a comprehensive study investigating the ability of modified theories of gravity in explaining the anomalous velocity dispersions of the ultra-diffuse galaxies. We choose three popular alternative theories of gravity: namely, Modified Newtonian gravity (MOND) [12, 13], Scalar-Tensor-Vector Gravity (STVG) or Modified Gravity (MOG) [14] and Weyl Conformal gravity [15, 16]. These three modified theories of gravity tries to explain the dynamics of galaxies and globular clusters without assuming the existence of the ‘exotic’ dark matter. These gravity theories successfully explain the observed rotation curves of a large number of galaxies ([17, 18] for MOND; [19–23] for Weyl gravity; [24–26] for MOG), dispersion profiles of galactic globular clusters ([27–29] for MOND; [30] for Weyl gravity; [31] for MOG) and the phenomenological RAR for galaxies ([23, 32] for MOND; [33] for Weyl gravity; [34] for MOG).

Previous studies [35–37] have shown that the current observation of DF2 (and DF4) are insufficient to rule out MOND scenarios while MOG is consistent with the quoted overall dispersion value in vD18a [38]. It has been further shown that the high velocity dispersions of DF44 is consistent with MOND expectation but at odds with MOG [39]. In our previous paper [1], we presented a Jeans analysis approach to investigate the velocity dispersions of DF2 and DF4 in the context of four modified theories of gravity (Weyl conformal gravity, MOND, MOG and Emergent gravity along with Newtonian gravity without dark matter). We showed that the radial dispersion data of DF2 (and the overall dispersion value of DF4) are consistent with these theories of gravity either in 2σ or 3σ confidence level. The analysis assumed the velocity anisotropy parameter ξ to be zero. In this paper, we would investigate while relaxing this assumption helps modified gravity theories to better match the observation. We further extend our study to the case of DF44 and explore the possible diversity of the velocity dispersion profiles of UDGs.

The rest of the paper is organized in the following way. We begin with a brief introduction of MOND, Weyl Conformal gravity and MOG (Section II). We then present the formulation of velocity dispersions in a spherically symmetric system like

arXiv:1910.09726v1 [gr-qc] 22 Oct 2019

*tousifislam24@gmail.com

ultra-diffuse galaxies (Section III). In the next section, we investigate the modified gravity theories in light of the observed velocity dispersions of DF2 (Section IV A) and DF44 (Section IV B); and then try to understand the possible diversity of the velocity dispersion profiles and the effects of the mass scale, length scale and anisotropy parameters on the dispersion profiles (Section IV C). We then present a preliminary study in Section IV D to understand whether RAR is consistent with DF2 and DF44. We finally discuss implications of the results, point out possible caveats of the analysis (Section V) and conclude (Section VI).

II. MODIFIED GRAVITY THEORIES

In this section, we provide an executive summary of Weyl Conformal gravity, MOND and MOG.

A. Weyl Conformal Gravity

Weyl conformal gravity [15, 16] is a covariant metric theory of gravity which employs the principle of local conformal invariance of the space-time. The action remains invariant under the transformation of the metric tensor $g_{\mu\nu}(x) \rightarrow \Omega^2(x)g_{\mu\nu}(x)$, where $\Omega(x)$ is a smooth strictly positive function. Such restrictions result an unique action

$$I_w = -\alpha_g \int d^4x \sqrt{-g} C_{\lambda\mu\nu\kappa} C^{\lambda\mu\nu\kappa}, \quad (2.1)$$

where α_g is a dimensionless coupling constant and $C_{\lambda\mu\nu\kappa}$ is the Weyl tensor [40]. The action leads to a fourth order field equation [16]:

$$4\alpha_g W^{\mu\nu} = 4\alpha_g (C^{\lambda\mu\nu\kappa}_{;\lambda\kappa} - \frac{1}{2} R_{\lambda\kappa} C^{\lambda\mu\nu\kappa}) = T^{\mu\nu}, \quad (2.2)$$

where $T^{\mu\nu}$ is the matter-energy tensor and ‘;’ denotes covariant derivative. It has been shown that, for a spherically symmetric mass distribution, the resultant acceleration of a test particle takes the following form [41, 42]:

$$a(r) = G \left[-\frac{I_0(r)}{r^2} + \frac{1}{R_0^2} \left(\frac{I_2(r)}{3r^2} - \frac{2}{3} r E_{-1}(r) - I_0(r) \right) \right] + \frac{GM_0}{R_0^2} - \kappa c^2 r. \quad (2.3)$$

where $I_n(r) = 4\pi \int_0^r \rho(x)x^{n+2}dx$ and $E_n(r) = 4\pi \int_r^{+\infty} \rho(x)x^{n+2}dx$ are the interior and exterior mass moments respectively. M_0 , R_0 and κ are three conformal gravity parameters. The numerical values of the parameters have been obtained through fitting galaxy rotation curves [19–22]: $R_0 = 24$ kpc and $M_0 = 5.6 \times 10^{10} M_\odot$ and $\kappa = 9.54 \times 10^{-54} \text{ cm}^{-2}$.

B. MOND

Modified Newtonian Dynamics (MOND) [12, 13] is a phenomenological theory of gravity which tries to explain the

observed galactic rotation curves by modifying the Newtonian acceleration law. The modification is achieved by introducing an interpolating function μ which projects the Newtonian acceleration a_N to the MOND acceleration a in the following way:

$$\mu \left(\frac{a}{a_0} \right) a = a_N. \quad (2.4)$$

The interpolating function $\mu(x) \approx x$ when $x \ll 1$ and $\mu(x) \approx 1$ when $x \gg 1$. Therefore, when the galactic gravitational field is strong, the MOND acceleration exhibits Newtonian behavior. The quantity a_0 is the critical value below which MOND deviates from Newtonian gravity. The exact functional form of the interpolating function $\mu(x = \frac{a}{a_0})$ is not fixed. In this paper, we would use the ‘standard’ form:

$$\mu(x) = \frac{x}{\sqrt{(1+x^2)}}, \quad (2.5)$$

where $a_0 = 1.14 \times 10^{-10} \text{ m/s}^2$. The MOND acceleration reads [12]

$$a_{MOND} = \frac{a_N}{\sqrt{2}} \left(1 + \left(1 + (2a_0/a_N)^2 \right)^{1/2} \right)^{1/2}, \quad (2.6)$$

where $a_N = \frac{GM(r)}{r^2}$ is the Newtonian acceleration generated through the baryonic mass.

The formulation presented above is strictly for the isolated MOND case for which the internal acceleration of the system a is much larger than the external field a_{ext} i.e. $a \gg a_{ext}$. When the external field becomes dominant ($a \ll a_{ext}$), one can safely ignore the internal field. However, when they are comparable, both must be taken into account. This particular effect, unique to MOND, is known as the External Field Effect (EFE) [35, 37]. To capture EFE appropriately, we modify the MOND acceleration law as:

$$(a + a_{ext}) \mu \left(\frac{a + a_{ext}}{a_0} \right) = a_N + a_{ext} \mu \left(\frac{a_{ext}}{a_0} \right). \quad (2.7)$$

One can then compute a if a_{ext} is known.

C. MOG

Scalar-Tensor-Vector Gravity (STVG) or the Modified Gravitational (MOG) theory is a covariant scalar-tensor-vector gravity theory which features a massive vector field ϕ_μ and three scalar fields G , μ and ω [14]. Instead of the Newtonian gravitational constant G_N , the theory allows a dynamical gravitational parameter G which varies with space and time. In this theory the acceleration within an arbitrary spherically symmetric mass distribution takes the following form:

$$a_{MOG} = - \int_0^r dr' \frac{2\pi G_N r'}{\mu r^2} \rho(r') \{ 2(1 + \alpha) + \alpha(1 + \mu r) [e^{-\mu(r+r')} - e^{-\mu(r-r')}] \} - \int_r^\infty dr' \frac{2\pi G r'}{\mu r^2} \rho(r') \alpha \times \{ (1 + \mu r) [e^{-\mu(r+r')} - (1 - \mu r) e^{-\mu(r-r')}] \} \quad (2.8)$$

where α and μ controls the strength and range of the attractive force, and G_N is the Newtonian gravitational constant. The

parameter α and μ depends on the mass scale of the system. The value of α is obtained from the relation

$$\alpha = \alpha_{\text{inf}} \frac{M}{(\sqrt{M} + E)^2}; \quad (2.9)$$

and μ is given by:

$$\mu = \frac{D}{\sqrt{M}}, \quad (2.10)$$

where $\alpha_{\text{inf}} = 10$, $D = 6.25 \times 10^3 M_{\odot}^{1/2} \text{ kpc}^{-1}$ and $E = 2.5 \times 10^4 M_{\odot}^{1/2}$ [43, 44].

III. JEANS ANALYSIS AND VELOCITY DISPERSION

We use the Jeans equation to estimate the velocity dispersion profile of a non-rotating system with spherically symmetric mass distribution (ultra-diffuse galaxies in our case) [45]. The equation reads:

$$\frac{\partial(\rho(r)\sigma^2(r))}{\partial r} + \frac{2\rho(r)\xi(r)\sigma^2(r)}{r} = \rho(r)a(r), \quad (3.1)$$

where r is the radial distance from the center of the object, $\rho(r)$ is the radial density function and $\xi(r)$ is the anisotropy parameter. The anisotropy parameter $\xi(r)$ is defined as:

$$\xi(r) = 1 - \frac{\sigma_{\theta}^2}{\sigma_r^2}, \quad (3.2)$$

with σ_{θ} and σ_r being the azimuthal and radial velocity dispersions respectively. In general, $\xi(r)$ is a function of r ; but for our analysis, we assume it to be constant. We also assume $\lim_{r \rightarrow \infty} \rho(r)\sigma^2(r) = 0$. It allows us to write:

$$\sigma^2(r) = \frac{1}{\rho(r)} \int_r^{\infty} \rho(r')a(r') \left(\frac{r'}{r}\right)^{2\xi} dr'. \quad (3.3)$$

The projected line-of-sight (LOS) velocity dispersion can then be written as:

$$\sigma_{\text{LOS}}^2(R) = \frac{\int_R^{\infty} \frac{r\sigma^2(r)\rho(r)}{\sqrt{r^2 - R^2}} dr - R^2 \int_R^{\infty} \frac{\xi\sigma^2(r)\rho(r)}{r\sqrt{r^2 - R^2}} dr}{\int_R^{\infty} r\rho(r)/\sqrt{r^2 - R^2} dr}, \quad (3.4)$$

where R is the projected distance from the center of the object.

TABLE I: **DF2: Reduced chi-square values as goodness-of-fits for different theories of gravity.** $D = 20.0 \text{ Mpc}$ and no dark matter are assumed.

	γ	β	χ^2/dof
Modified Gravitational Theory (MOG)	2.0	-1.0	1.10
Modified Newtonian Dynamics (MOND)	2.0	0.95	3.01
MOND with EFE	0.7	-0.99	1.40
Weyl Conformal Gravity	1.0	0.95	3.06
GR (without DM)	2.5	-1.0	1.46

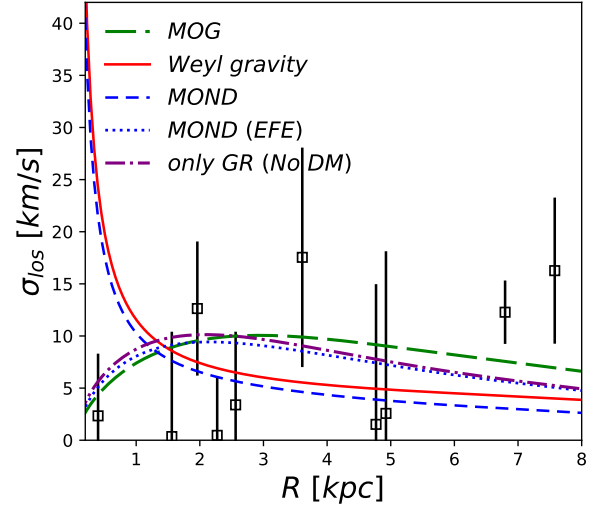


FIG. 1: **Line-of-sight velocity dispersion profile of NGC1052-DF2:** The black squares with error-bars denote the individual dispersion measurement. On top of these, we plot the best-fit Weyl gravity dispersion profile in red solid line, MOND profile in short dashed blue line, MOND with EFE in dotted blue line and MOG profile in long dashed green. For the GR profile (magenta dash dotted line), we assume no dark matter.

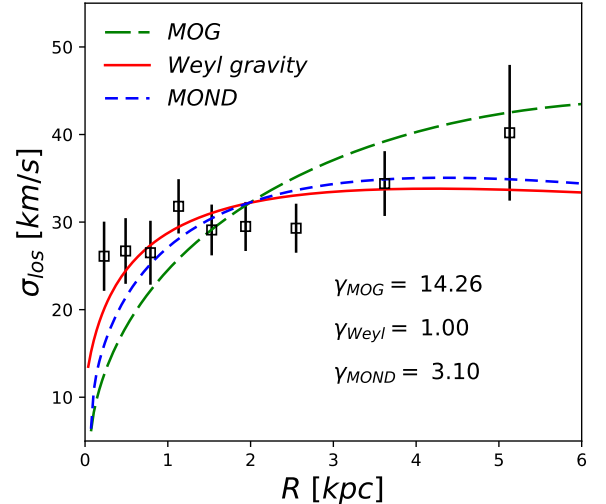


FIG. 2: **Line-of-sight velocity dispersion profile of NGC1052-DF44:** The black squares with error-bars denote the individual dispersion measurements. On top of these, we plot the best-fit Weyl gravity dispersion profile in red solid line, MOND profile in short dashed blue line and MOG profile in long dashed green. For the GR profile (magenta dash dotted line), we assume no dark matter.

IV. RESULTS

A. Extreme Case I : NGC 1052-DF2

The surface brightness of the ultra-diffuse galaxy NGC1052-DF2 can be modelled using a two-dimensional Sérsic profile, with index $n = 0.6$, effective radius $R_e = 2.2 \text{ kpc}$ and total luminosity $L = 1.2 \times 10^8 L_{\odot}$ [2]. This indicates a total mass of $M \sim 2.0 \times 10^8 M_{\odot}$ within a radius 7.6 kpc (assuming standard

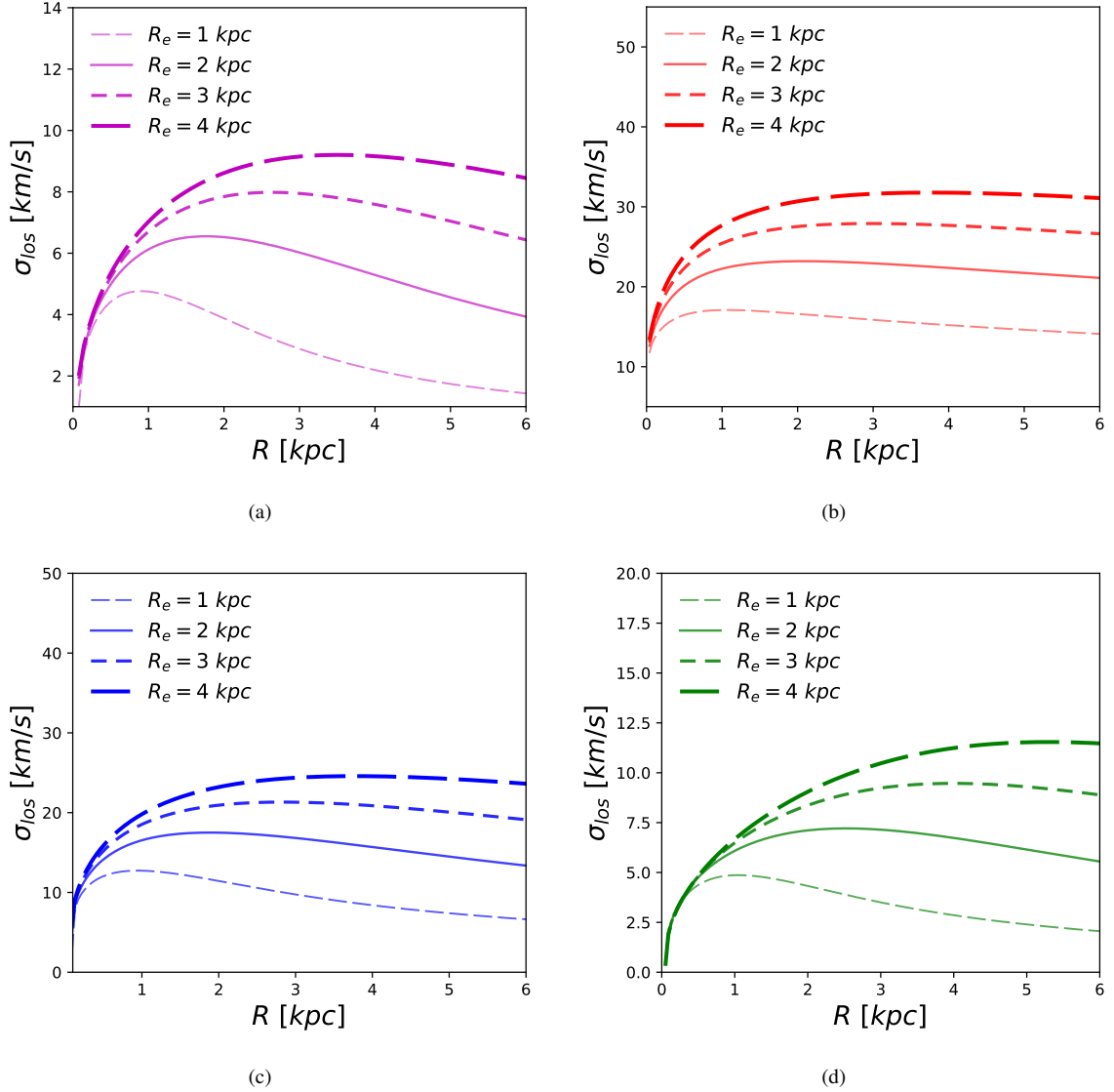


FIG. 3: The figure depicts the diversity of dispersion profiles resulted from different values of the effective radius in the context of four different theories of gravity: GR (in panel (a)), Weyl gravity (in panel (b)), MOND (in panel (c)) and MOG (in panel (d)). While GR and Weyl gravity profiles are plotted in magenta and red respectively, we use blue and green to represent MOND and MOG profiles respectively. We choose four different values of the effective radius: $R_e = [1, 2, 3, 4]$ kpc. Color codes are given in legends. (Section IV C in text)

stellar population modelling). The resultant mass density can be closely approximated as [38]:

$$\rho_{ser} = \gamma \frac{20\Sigma_0}{63R_e} \exp\left[-\left(\frac{11r}{10R_e}\right)^{4/3}\right], \quad (4.1)$$

where γ is the mass-to-light ratio, $\Sigma_0 = 1.25 \times 10^7 M_\odot/kpc^2$ is the characteristic surface mass density and $R_e = 2.0$ kpc is the effective radius.

We first present a comparison between the data [11] and the best-fit line-of-sight (los) velocity dispersion profiles in modified gravity theories in Figure 1. The individual GC velocity dispersion measurements are shown in black squares along with their quoted error-bars. We assume a distance (from us) $D = 20$ Mpc and allow the mass-light ratio γ and anisotropy ξ to vary. Additionally, we impose a sharp trimming of the mass profile at $r_{cut} = 10$ kpc to model tidal stripping of DF2 due to nearby massive galaxies. In MOND, within the context of EFE, the external acceleration due to the host NGC 1052

is $a_{ext} \sim 0.15a_0$. We set $a_{ext} = 0.15a_0$ to compute the effective MOND profile with EFE. The resultant best-fit modified gravity dispersion profiles from the inferred baryonic mass (long dash dotted magenta line for GR; solid red line for Weyl gravity; short dashed blue line for MOND; dotted blue line for MOND with EFE and long dashed green line for MOG) are then superimposed in Figure 1. The best-fit parameter values and the corresponding reduced chi-square values are reported in Table I. We find that while MOG, MOND with EFE and GR (without DM) favour a model with highly negative anisotropy, Weyl gravity and MOND prefers positive values of ξ . The later two theories exhibit a high mismatch in the interior of the DF2. Though the chi-square values of Weyl gravity and MOND are slightly higher than GR and MOG, we find that all four theories in question can reasonably fit the dispersion data with acceptable mass-to-light ratio. It is important to note that the galaxy is considered to be devoid of ‘dark matter’ in the Λ CDM context. Therefore, GR (without DM) should be

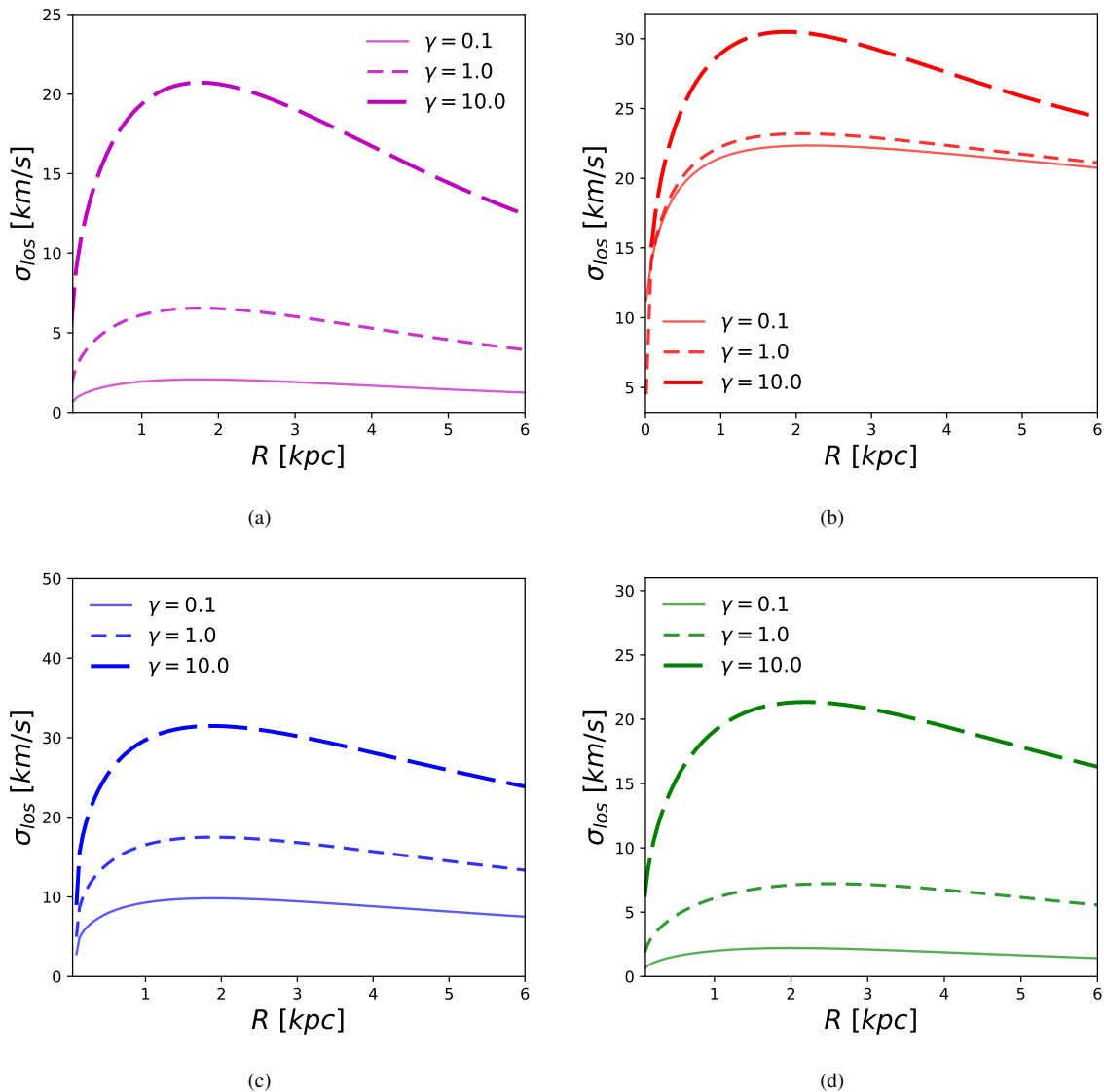


FIG. 4: The figure depicts the diversity of dispersion profiles resulted from different values of the mass-light ratios in the context of four different theories of gravity: GR (in panel (a)), Weyl gravity (in panel (b)), MOND (in panel (c)) and MOG (in panel (d)). While GR and Weyl gravity profiles are plotted in magenta and red respectively, we use blue and green to represent MOND and MOG profiles respectively. We choose three different values of the mass-light ratio: $\gamma = [0.1, 1.0, 10.0]$. Color codes are given in the legends. (Section IV C in text)

able to fit the data. This is the reason we also show best-fit GR (without DM) profile in Figure 1.

B. Extreme Case II : NGC 1052-DF44

DF44 is very similar to DF2 in terms of size and luminosity. However, it shows an extraordinary high velocity dispersions of $\sigma \sim 41.0 \pm 8$ km/s [5]. For DF44, we assume a mass profile similar to DF2 (Eq. 4.1) but with the characteristic surface mass density $\Sigma_0 = 0.686 \times 10^7 M_\odot/kpc^2$ and effective radius $R_e = 4.6$ kpc. For this galaxy, we use $r_{cut} = 20$ kpc. This particular galaxy is considered to be a dark matter dominated galaxy with little baryonic contents in the context of Λ CDM. Thus, only GR (without DM) model would not be able to fit the data. We therefore do not intent to find a best-fit model for GR (without DM). In Figure 2, we show the best-fit modified gravity dispersion profiles along with observed values.

The best-fit mass-to-light ratios for Weyl gravity, MOND and MOG are shown in Table II. We fix the anisotropy $\xi = -0.5$. This choice of ξ is consistent with the results of Haghi *et al* [39] and Bilek *et al* [46].

TABLE II: DF44: Reduced chi-square values as goodness-of-fits for different theories of gravity. No dark matter are assumed.

	γ	χ^2/dof
Modified Gravitational Theory (MOG)	14.26	3.65
Modified Newtonian Dynamics (MOND)	3.10	1.76
Weyl Conformal Gravity	1.00	0.84

We observe that the best-fit mass-to-light ratio γ for Weyl gravity ($\gamma_{weyl} = 1.0$) and MOND ($\gamma_{MOND} = 3.1$) are acceptable for UDGs and matches with the estimates from population synthesis and stellar evolution models [39]. On the other hand, MOG requires unacceptably high mass-to-light ratio

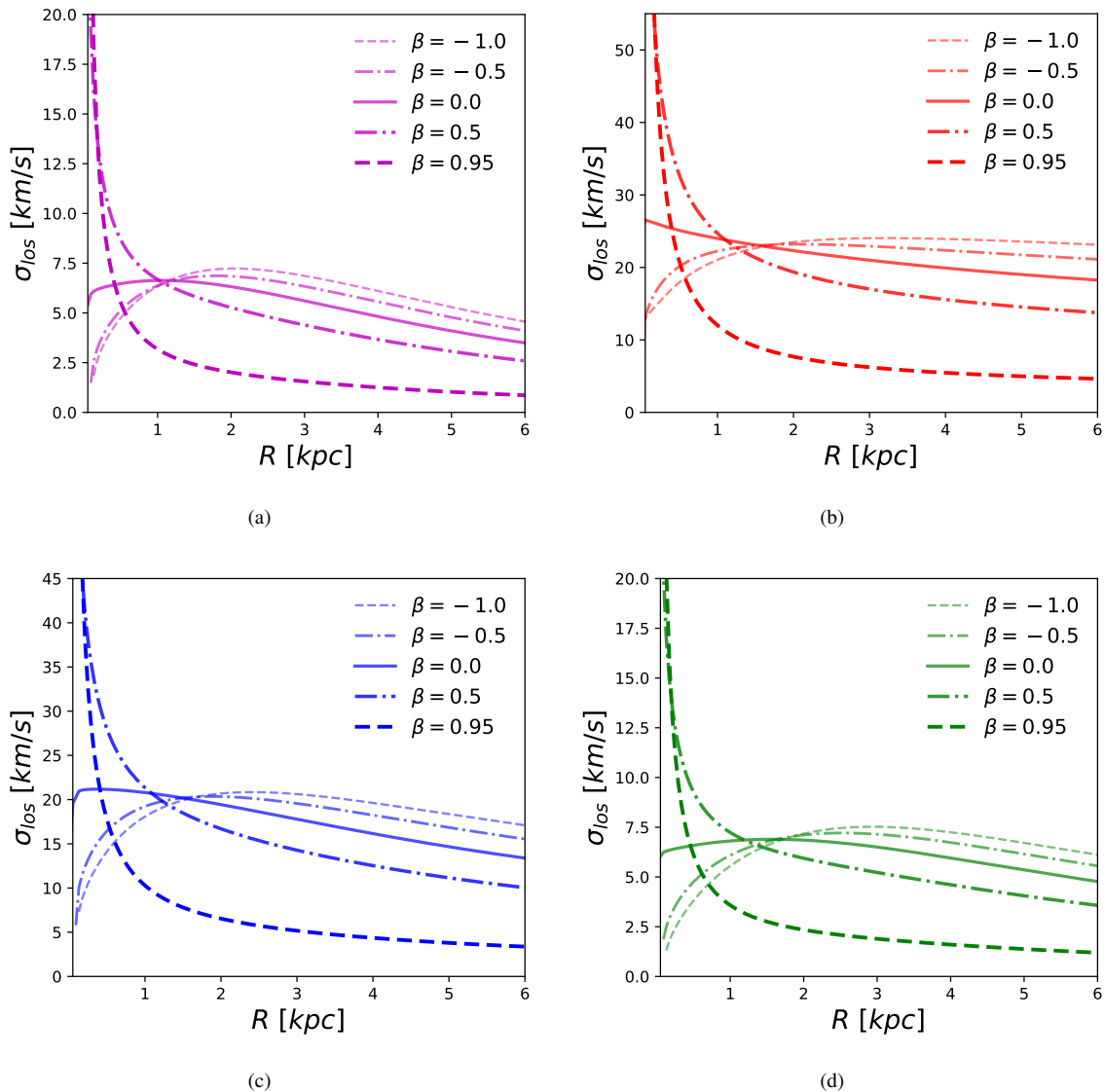


FIG. 5: The figure depicts the diversity of dispersion profiles resulted from different values of the anisotropy parameter in the context of four different theories of gravity: GR (in panel (a)), Weyl gravity (in panel (b)), MOND (in panel (c)) and MOG (in panel (d)). While GR and Weyl gravity profiles are plotted in magenta and red respectively, we use blue and green to represent MOND and MOG profiles respectively. We choose five different values for the anisotropy parameter: $\beta = [-1.0, -0.5, 0.0, 0.5, 0.95]$. Color codes are given in legends. (Section IV C in text)

($\gamma_{MOG} = 14.26$) to fit the observed dispersion profile. Thus, we conclude that MOG is not consistent with DF44 while it can fit DF2 very well. Therefore, the anomaly of DF2 and DF44 together sets a challenge for MOG. Weyl gravity and MOND, however, are found to be able to account for both the enigmatic galaxies (DF2 and DF44). For DF44, we do not take EFE into consideration as no massive nearby galaxy, that might generate an external field for DF44, has been reported.

C. Possible Diversity of Dispersion profiles in Modified gravity

The observations of the anomalous velocity dispersions of DF2 and DF44 are also important because they represent the extreme ends of baryon-dark matter relative contents in a galaxy within the framework of Λ CDM. While DF2 consists of mostly baryons, DF44 is made of mostly ‘dark matter’.

Though these two galaxies are similar to each other in many senses, their dispersion profiles have little similarity. While in Λ CDM, such extreme observations can be accommodated by tuning the dark matter contents in each galaxy, modified gravity theories lack any such luxury. We should therefore investigate how much diversity one can accommodate in dispersion profiles of UDGs in modified gravity theories.

To understand the possible diversity, we consider a toy galaxy which follows a mass profile described in Eq. 4.1. We then take the following strategy:

1. We set the mass-to-light ratio $\gamma = 2.0$, anisotropy $\xi = -0.5$ and $r_{cut} = 20$ kpc; and vary the effective radius R_e . We choose four different values of $R_e = [1.0, 2.0, 3.0, 4.0]$ kpc.
2. We then fix R_e to be 2.0 kpc and vary the mass-to-light ratio $\gamma = [0.1, 1.0, 10.0]$. All other parameters are kept unchanged.

3. Finally, we decide to vary the anisotropy parameter ξ . We explore five different values: $\xi = [-1.0, -0.5, 0.0, 0.5, 0.95]$.

Throughout this exercise, we keep the characteristic surface mass density $\Sigma_0 = 1.25 \times 10^7 M_\odot/kpc^2$ unchanged. This approach allows us to explore the effects of the mass scale (γ), length scale (R_e) and anisotropy parameter (ξ) on the observed velocity dispersion profiles. In Figure 3, we plot the resultant velocity dispersion profiles in Weyl gravity, MOG and (isolated) MOND with different input values for the effective radius R_e . We also show the corresponding GR (without DM) profile for comparison. The diversity due to varying mass-light ratio γ and anisotropy ξ have been shown in Figure 4 and Figure 5 respectively. We observe that obtained dispersion profiles show all kinds of features (increasing; declining; increasing followed by a monotonic decline; increasing followed by a flat plateau). Furthermore, features due to different values of a particular model parameter (e.g. ξ) are almost same across theories with some exceptions. For example, we find varying mass-to-light ratio results different dispersion profiles which are well separated in MOND or MOG. However, in Weyl gravity, the dispersion profiles for smaller values of γ shows a converging trend. This is because, in Weyl gravity, both local and global effects contribute to the internal dynamics (differently from EFE in MOND). The second and third term in Equation 2.3 refers to the contribution from the global mass distribution (we refer the readers to [16] for a comprehensive review). The third term in Equation 2.3 generates a constant acceleration while the fourth term is negligible at the galactic scale. The constant term ($\frac{GM_0}{R_0^2}$) directs the dispersion profiles to converge to particular values when we keep decreasing the mass-light ratio γ .

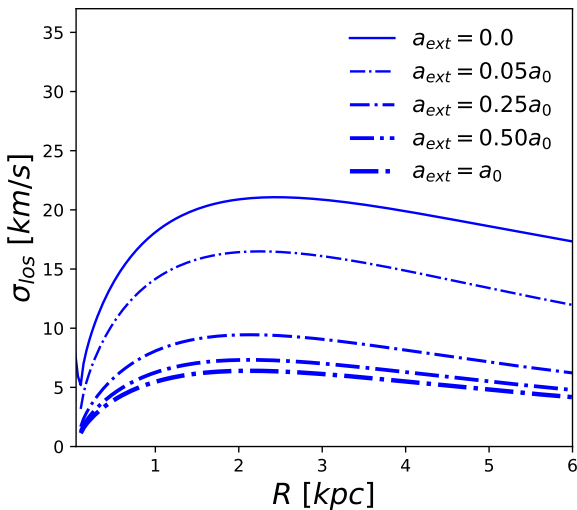


FIG. 6: The figure depicts the diversity of dispersion profiles in MOND resulted from different values of the external field strength. Color codes are given in the legend. (Section IV C in text)

For the sake of completeness, we now present Figure 6 where we show different dispersion profiles when the toy galaxy is immersed in external fields with different strengths. We assume the effective radius $R_e = 2$ kpc and anisotropy $\xi = -1.0$. We explore the kinematics for a set of five different values of external field strength: $a_{ext} =$

$\{0.0, 0.05a_0, 0.25a_0, 0.5a_0, a_0\}$. We find that the presence of an external field can significantly reduce the dispersion velocities in a MOND scenario.

This study of systematics in the velocity dispersion profiles indicates that it is possible to explain different kinds of dispersion profiles for UDGs in modified gravity theories. Future availability of dispersion data of other UDGs would thus provide exciting tests for the ability of modified gravity theories to accommodate diverse features.

D. Do UDGs follow Radial Acceleration Relation (RAR) ?

Analysis of 153 spiral galaxies by McGaugh *et al* [10] revealed tighter correlation between the radial acceleration inferred from the rotation curves of galaxies and the same expected from Newtonian (centripetal) acceleration generated by the baryons. This empirical relation, known as Radial Acceleration Relation (RAR), is given by:

$$a_{RAR} = \frac{a_n}{1 - \exp(-(\frac{a_n}{a^\dagger})^{1/2})}, \quad (4.2)$$

where a_n is the Newtonian acceleration produced by the baryonic mass only and $a^\dagger = 1.2 \times 10^{-10} m/s^2$ is the acceleration scale. Lelli *et al* [47] have further found that similar relation holds for other types of galaxies such as ellipticals, lenticulars, and dwarf spheroidals. The universality of RAR across different types of galaxies is considered to be an indication of an underlying departure from GR at the galactic scale. In this section, we would like to find out whether the RAR scaling holds true for DF2 and DF44 too.

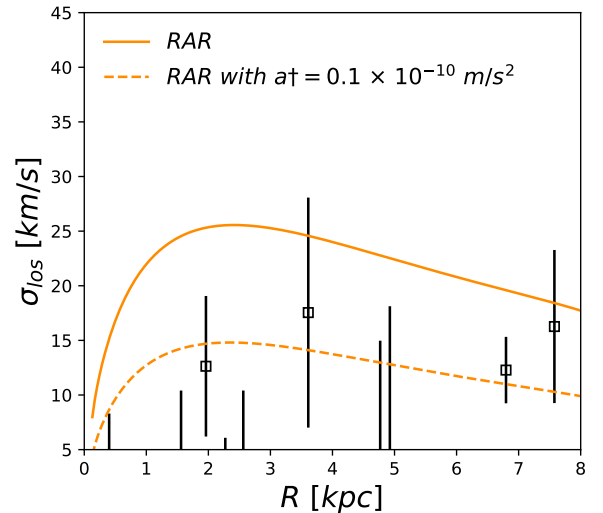


FIG. 7: Line-of-sight velocity dispersion profile of NGC1052-DF2 and RAR: The black squares with error-bars denote the individual dispersion measurements. On top of these, we plot the predicted RAR dispersion profile in orange solid line.

To investigate this direction, we first replace the acceleration law by Eq. 4.2 and compute the velocity dispersion profiles for DF2 and DF44. In case of DF2, we assume $\gamma = 2.0$ and $\xi = -1.0$ (in accordance with the best-fit GR without DM profile). For DF44, we fix $\gamma = 1.3$ and $\xi = -0.5$. In Figure 7, we plot the resultant dispersion profile from RAR

scaling along with observed values (black square) for DF2. It is clear that RAR fails to account for the observed profile with its universal acceleration scale $a\ddagger = 1.2 \times 10^{-10} \text{ ms}^{-2}$ (solid orange line). However, a smaller value of $a\ddagger$ ($0.1 \times 10^{-10} \text{ ms}^{-2}$) is able to yield a good match with data (dashed orange line). On the other hand, RAR does an excellent job in fitting DF44 dispersion data with the original acceleration scale $a\ddagger = 1.2 \times 10^{-10} \text{ ms}^{-2}$. The resultant RAR profile goes through several of the DF44 dispersion data-points (Figure 8).

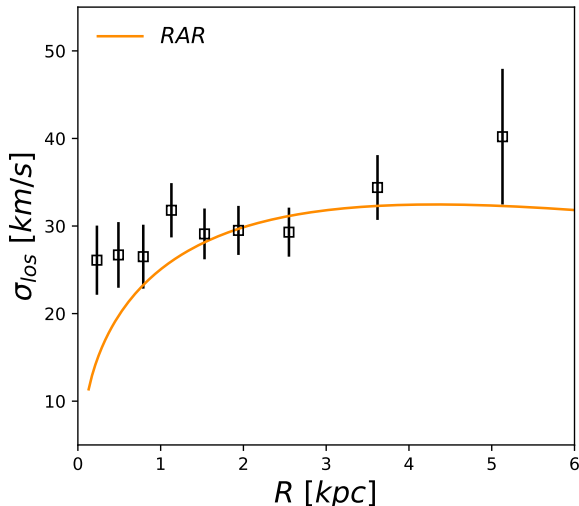


FIG. 8: **Line-of-sight velocity dispersion profile of NGC1052-DF44 and RAR:** The black squares with error-bars denote the individual dispersion measurements. On top of these, we plot the predicted RAR dispersion profile in orange solid line.

V. DISCUSSIONS

In our previous paper [1] we test four modified theories of gravity (namely Weyl conformal gravity, MOND, MOG and Emergent gravity along with GR without dark matter) to explore whether it is possible to explain the dynamics of DF2 and DF4 in the context of modified gravity theories. Our analysis suggested that, except for Emergent gravity, it is possible to fit the observed dispersion data of these UDGs with reasonable success in modified gravity paradigm. Our study assumed the anisotropy parameter to be zero throughout - an assumption which might not be true always. In this paper, we have relaxed this particular assumption and allowed anisotropy parameter ξ to take non-zero values. In fact, as we show in Section IV C, different values of ξ results in diverse features in the velocity dispersion profiles. We further observe that all theories studied in [1] prefer to assume a non-zero value for the best-fit profiles.

Haghi *et al.* [39] have also examined the viability of MOG and MOND using the radial dispersion data of DF44. For MOG, they followed two different approaches. First, they fixed the value of the two MOG parameters μ and α to the values obtained from rotation curve fits [24]. A fit to the data requires a high mass-to-light ratio of $\gamma = 7.4$, inconsistent with stellar population synthesis models. The authors then allowed μ and α to vary resulting best-fit values of $\alpha = 221 \pm 112$ and $\mu = 0.41 \pm 35 \text{ kpc}^{-1}$. These values are significantly larger than

the values obtained from galactic rotation curve surveys. We, however, took a different strategy in our analysis. Instead of treating μ and α to be completely independent, we use their dependences on the mass and length scale (Eq. 2.9 and Eq. 2.10) to infer their true values in the systems like DF2 and DF44 - an approach recommended by Moffat and Toth [38].

Our analysis do not explicitly incorporate any effect of tidal heating. However, we use a simplistic way to compensate the effects of tidal stripping (if any) due to nearby massive galaxies. We assume a phenomenological cut-off radius r_{cut} beyond which we set the mass density to be zero. For DF2, we use $r_{\text{cut}} = 10 \text{ kpc}$ (taking into account that the last observed GC lies about 8 kpc from the galactic center and the host (massive) galaxy NGC 1052 is only 80 kpc away). For DF44, however, we use to larger value of $r_{\text{cut}} = 20 \text{ kpc}$ as no nearby massive galaxy has been reported. We further assume the distance of DF2 to be 20 Mpc. However, [48] reports a different estimation of $D \sim 13.2 \text{ Mpc}$. We have already showed in our previous analysis [1] that a closer distance results a better match between data and modified gravity models.

Furthermore, we have explored the External Field Effects (EFE) [35] in MOND in addition to isolated MOND computations. We find that MOND better matches the dispersion data when EFE is included. However, EFE could be safely neglected for DF44 [39] due to the same reason we set a larger value for r_{cut} for this galaxy.

VI. CONCLUSIONS

In this paper, we investigated the viability of three popular modified gravity theories (Weyl conformal gravity, MOND and MOG) in the light of recent observations of anomalous velocity dispersion of NGC 1052-DF2 and NGC 1052-DF44. The first galaxy exhibits an extremely low velocity dispersion compared to its radial extent while the second galaxy has quite high dispersion values. In fact, these two galaxies mark the two extreme ends among known galaxies in terms of estimated dynamical mass (or apparent ‘dark matter’ contents in ΛCDM). We find that Weyl gravity and MOND manages to fit the dispersion profiles reasonably without the need of any dark matter for both the galaxies. MOG, on the other hand, can explain the observed dispersion of DF2 easily but fails to account for DF44 unless it assumes high mass-to-light ratio (i.e., in other words, unless it assumes some amount of dark matter).

We further showed that, within the context of modified gravity theories, the UDGs (and other galaxies) can accommodate diverse features in the dispersion profiles. This result is intriguing in the sense that while ΛCDM model typically does this job by fine-tuning the dark matter halo parameters (and other typical galactic parameters concerning morphology), modified gravity theories can achieve the same goal with less number of freedom in their structures.

Finally, we present a preliminary investigation of whether the celebrated ‘Radial Acceleration Relation’ (RAR), documented in hundreds of galaxies, between expected Newtonian acceleration and observed radial acceleration holds true for DF2 and DF44. We have found that while DF44 complies with RAR with the original acceleration scale $a\ddagger = 1.2 \times 10^{-10} \text{ ms}^{-2}$, DF2 follows the same relation but with a different value of the acceleration scale $a\ddagger$. In future, as more and more

dispersion data for UDGs would be available, it would be exciting to statistically analyze the compatibility between RAR and UDGs.

Acknowledgement: TI thanks Koushik Dutta for fruitful dis-

cussions and UMass Dartmouth for support through Doctoral Fellowship. Computation has been carried out in the cluster CARNIE at Center for Scientific Computation and Visualization Research (CSCVR), University of Massachusetts (UMass) Dartmouth.

-
- [1] T. Islam and K. Dutta, arXiv preprint arXiv:1908.07160 (2019).
- [2] P. Van Dokkum, S. Danieli, Y. Cohen, A. Merritt, A. J. Romanowsky, R. Abraham, J. Brodie, C. Conroy, D. Lokhorst, L. Mowla, et al., *Nature* **555**, 629 (2018).
- [3] P. van Dokkum, Y. Cohen, S. Danieli, A. Romanowsky, R. Abraham, J. Brodie, C. Conroy, J. Kruijssen, D. Lokhorst, A. Merritt, et al., arXiv preprint arXiv:1806.04685 (2018).
- [4] P. van Dokkum, S. Danieli, R. Abraham, C. Conroy, and A. J. Romanowsky, *The Astrophysical Journal Letters* **874**, L5 (2019).
- [5] P. van Dokkum, R. Abraham, J. Brodie, C. Conroy, S. Danieli, A. Merritt, L. Mowla, A. Romanowsky, and J. Zhang, *The Astrophysical Journal* **828**, L6 (2016), URL <https://doi.org/10.3847%2F2041-8205%2F828%2FL6>.
- [6] A. Nusser, arXiv preprint arXiv:1907.08035 (2019).
- [7] G. Ogiya, *Monthly Notices of the Royal Astronomical Society: Letters* **480**, L106 (2018).
- [8] N. Leigh and G. Fragione, arXiv preprint arXiv:1903.06717 (2019).
- [9] J. Silk, arXiv preprint arXiv:1905.13235 (2019).
- [10] S. S. McGaugh, F. Lelli, and J. M. Schombert, *Physical Review Letters* **117**, 201101 (2016).
- [11] A. Wasserman, A. J. Romanowsky, J. Brodie, P. van Dokkum, C. Conroy, R. Abraham, Y. Cohen, and S. Danieli, *The Astrophysical Journal Letters* **863**, L15 (2018).
- [12] M. Milgrom, *The Astrophysical Journal* **270**, 365 (1983).
- [13] B. Famaey and S. S. McGaugh, *Living reviews in relativity* **15**, 10 (2012).
- [14] J. W. , *Journal of Cosmology and Astroparticle Physics* **2006**, 004 (2006).
- [15] P. D. Mannheim and D. Kazanas, *The Astrophysical Journal* **342**, 635 (1989).
- [16] P. D. Mannheim, *Progress in Particle and Nuclear Physics* **56**, 340 (2006).
- [17] R. H. Sanders and S. S. McGaugh, *Annual Review of Astronomy and Astrophysics* **40**, 263 (2002).
- [18] G. Gentile, B. Famaey, and W. de Blok, *Astronomy & Astrophysics* **527**, A76 (2011).
- [19] P. D. Mannheim and J. G. O'Brien, *Physical Review D* **85**, 124020 (2012).
- [20] P. D. Mannheim, *The Astrophysical Journal* **479**, 659 (1997).
- [21] P. D. Mannheim and J. G. O'Brien, *Physical review letters* **106**, 121101 (2011).
- [22] J. G. O'Brien and P. D. Mannheim, *Monthly Notices of the Royal Astronomical Society* **421**, 1273 (2012).
- [23] K. Dutta and T. Islam, *Phys. Rev. D* **98**, 124012 (2018).
- [24] J. Moffat and S. Rahvar, *Monthly Notices of the Royal Astronomical Society* **436**, 1439 (2013).
- [25] J. Moffat and V. Toth, *Physical Review D* **91**, 043004 (2015).
- [26] J. Moffat and V. T. Toth, arXiv preprint arXiv:1103.5634 (2011).
- [27] R. Scarpa, G. Marconi, and R. Gilmozzi, *Astronomy & Astrophysics* **405**, L15 (2003).
- [28] R. Scarpa, G. Marconi, and R. Gilmozzi, arXiv preprint astro-ph/0411078 (2004).
- [29] R. Scarpa, G. Marconi, R. Gilmozzi, and G. Carraro, *Astronomy & Astrophysics* **462**, L9 (2007).
- [30] T. Islam, arXiv preprint arXiv:1811.00065 (2018).
- [31] J. Moffat and V. Toth, *The Astrophysical Journal* **680**, 1158 (2008).
- [32] A. Ghari, H. Haghi, and A. H. Zonoozi, *Monthly Notices of the Royal Astronomical Society* **487**, 2148 (2019).
- [33] J. G. O'Brien, T. L. Chiarelli, P. D. Mannheim, M. A. Falcone, M. H. AlQurashi, and J. Carter, in *Journal of Physics: Conference Series* (IOP Publishing, 2019), vol. 1239, p. 012009.
- [34] M. Green and J. Moffat, *Physics of the Dark Universe* **25**, 100323 (2019).
- [35] B. Famaey, S. McGaugh, and M. Milgrom, *Monthly Notices of the Royal Astronomical Society* **480**, 473 (2018).
- [36] P. Kroupa, H. Haghi, B. Javanmardi, A. H. Zonoozi, O. Müller, I. Banik, X. Wu, H. Zhao, and J. Dabringhausen, *Nature* **561**, E4 (2018).
- [37] H. Haghi, P. Kroupa, I. Banik, X. Wu, A. H. Zonoozi, B. Javanmardi, A. Ghari, O. Müller, J. Dabringhausen, and H. Zhao, *Monthly Notices of the Royal Astronomical Society* **487**, 2441 (2019).
- [38] J. Moffat and V. Toth, *Monthly Notices of the Royal Astronomical Society: Letters* **482**, L1 (2018).
- [39] H. Haghi, V. Amiri, A. H. Zonoozi, I. Banik, P. Kroupa, and M. Haslbauer, arXiv preprint arXiv:1909.07978 (2019).
- [40] H. Weyl, *Mathematische Zeitschrift* **2**, 384 (1918).
- [41] K. Horne, *Monthly Notices of the Royal Astronomical Society* **369**, 1667 (2006).
- [42] A. Diaferio and L. Ostorero, *Monthly Notices of the Royal Astronomical Society* **393**, 215 (2009).
- [43] J. Moffat and V. Toth, *The Astrophysical Journal* **680**, 1158 (2008).
- [44] J. Moffat and V. T. Toth, *Classical and Quantum Gravity* **26**, 085002 (2009).
- [45] J. Binney and S. Tremaine, *Galactic dynamics, princeton univ* (1987).
- [46] M. Bílek, O. Müller, and B. Famaey, *Astronomy & Astrophysics* **627**, L1 (2019).
- [47] F. Lelli, S. S. McGaugh, J. M. Schombert, and M. S. Pawłowski, *The Astrophysical Journal* **836**, 152 (2017).
- [48] I. Trujillo, M. A. Beasley, A. Borlaff, E. R. Carrasco, A. Di Cintio, M. Filho, M. Monelli, M. Montes, J. Román, T. Ruiz-Lara, et al., *Monthly Notices of the Royal Astronomical Society* **486**, 1192 (2019).